

## Effect of carrier materials on the properties of the andrographolide solid dispersion

Shoude Zhang<sup>1+</sup>, Qingyun Zeng<sup>1+</sup>, Guowei Zhao<sup>1\*</sup>, Wei Dong<sup>1</sup>,  
Liquan Ou<sup>1</sup>, Ping Cai<sup>1</sup>, Zhenggen Liao<sup>1</sup>, Xinli Liang<sup>1</sup>

<sup>1</sup>Key Laboratory of Modern Preparation of Traditional Chinese Medicine, Ministry of Education, Jiangxi University of Traditional Chinese Medicine, China

+ These authors contributed equally to this work.

In the work the andrographolide (AG)-solid dispersions (SDs) were prepared by the spray-drying method, using polyethylene glycol 8000 (PEG8000), Poloxamer188, polyvinylpyrrolidone K30 (PVPK30), Soluplus<sup>®</sup> as carrier materials. The effect of different polymers as carrier materials on the properties of the AG-SDs were studied. The results showed obvious differences in intermolecular interaction, thermal stability, drug state, powder properties, dissolution behavior, and so on of AG-SDs prepared using different polymers as carrier materials. AG-PEG8000-SD was a partial-crystalline and partial-amorphous powder with smaller surface area and pore volume, but it was easy to wetting and did not swell in contact with dissolved medium. AG-Soluplus<sup>®</sup>-SD was completely amorphous powder with larger specific surface area and pore volume, but it swelled in contact with water. Therefore, the dissolution profile of AG in AG-PEG8000-SD was similar to that in AG-Soluplus<sup>®</sup>-SD. Soluplus<sup>®</sup> and PEG8000 were suitable polymers to design AG-SDs, considering both physicochemical properties and dissolution behaviors. The results of this research showed that when selecting carrier materials for SD, we should not only consider the state of drugs in SD and the powder properties of SD, but also consider whether there is swelling when the carrier materials are in contact with the dissolution medium.

**Keywords:** Andrographolide. Solid dispersion. Physicochemical properties. Dissolution.

### INTRODUCTION

Over 40% of active pharmaceutical ingredients in development pipelines are poorly water-soluble drugs which limits formulation approaches, clinical application and marketability because of their low dissolution and bioavailability (Zhang *et al.*; 2015; FDA, 2000). Solid dispersion (SD) is used as a useful approach to improve the solubility, dissolution rate and bioavailability of poorly water-soluble active pharmaceutical ingredients (Chiou, Riegelman, 1971; Bikiaris *et al.*, 2005; Chokshi *et al.*, 2007; Kawabata *et al.*, 2011; Vo, Park, Lee, 2013; Singh *et al.*, 2017; Hu, Lou, Hageman, 2018; Zhao *et al.*,

2019). The poorly water-soluble drugs in solid dispersion can be dispersed as separate molecules, amorphous particles, or crystalline particles. Solid dispersion has many advantageous properties in improving the solubility and dissolution rate of poorly water-soluble drugs. These advantageous properties include changing of the drug crystal structure into an amorphous structure, reducing particle size and aggregation, enhancing wettability and porosity, and so on.

Most of the carrier materials used in solid dispersions are polymers, such as polyethylene glycol (PEG), poloxamer, polyvinylpyrrolidone (PVP), Soluplus<sup>®</sup>, and so on (Reginald-Opara *et al.*, 2015; Barmpalexis *et al.*, 2013; Mahmah *et al.*, 2014; Thenmozhi, Yoo, 2017; Eloy, Marchetti, 2014; Chutimaworapan *et al.*, 2000; Ramadhani *et al.*, 2014; Thiry *et al.*, 2016). The carrier material has an important influence on the

\*Correspondence: G. Zhao. Key Laboratory of Modern Preparation of Traditional Chinese Medicine. Ministry of Education. Jiangxi University of Traditional Chinese Medicine. Nanchang 330004, China. Phone: +86-791-87118658. E-mail: weiweihaoyunqi@163.com.

existing state and dissolution behavior of the drug in SD, thermal properties and powder properties of SD, and so on. PEG is widely used in solid dispersion owing to its low melting point, excellent solubility in water or organic solvents, low toxicity and low cost. PEG is very suitable for the preparation of SDs by the melting method and the solvent method. PVPK-30 is a high-molecular-weight water-soluble polymer, its high viscosity can prevent the recrystallization of drugs in the preparation, storage and dissolution process. Poloxamer is nonionic surfactants and polyvinyl caprolactam–polyvinyl acetate–polyethylene glycol graft copolymer (Soluplus®) is slightly surface-active, this property can be useful to maintain supersaturation of poorly soluble drugs in the gastrointestinal tract. It is generally believed that the drug in SD exists in amorphous state, and the SD powder has a large specific surface area and pore volume, which is beneficial to the dissolution of the drug in SD. Therefore, in this work, SDS were prepared using different polymers as carrier materials, and the effects of different polymers on the physicochemical properties and solubility behavior of the SDs were studied to find a suitable polymer for the application of SDs.

*Andrographis paniculata* (Burm. F.) Nees. is a herbaceous medicinal plant in the family of Acanthaceae and is native to China, India and other southeast Asian countries. The aerial parts (stems and leaves) of *Andrographis paniculata* have been widely used to treat internal body heat, common cold, non-infectious diarrhea, inflammation, herpes, sore throat and a variety of other chronic infectious diseases. Andrographolide (AG), a diterpenoid lactone, is the primary bioactive constituent of *Andrographis paniculata*, and has proven to be mainly responsible for the therapeutic properties of this herbal medicine. AG has many pharmacological actions, such as analgesic, antipyretic, anti-inflammatory, anti-infection, antiviral, anticancer, anti-hyperglycemia, anti-angiogenesis, immunostimulation, hepato-protection, antifertility and anti-HIV effects. The potential use of AG has attracted wide attention in recent years. However, AG is a colorless and crystalline bicyclic compound, sparingly soluble in water. It has high lipophilicity ( $\log P = 2.63$ ) and low aqueous solubility ( $74 \mu\text{g/mL}$ ). The therapeutic use of AG is restricted by its poor solubility

in water which results in low bioavailability after oral administration (Zhang *et al.*, 2015; Matsuda *et al.*, 1994; Calabrese *et al.*, 2000; Zhang, Tan, 2000; Shen *et al.*, 2002; Singha, Roy, Dey, 2007; Sermkaew *et al.*, 2013; Wen *et al.*, 2014; Jiang *et al.*, 2014). Therefore, AG was chosen as the model drug in this work.

In this paper, the AG-SDs were prepared by the spray-drying method (Bhardwaj *et al.*, 2018; Marasini *et al.*, 2013; Thybo *et al.*, 2008), using PEG8000, Poloxamer188, PVPK30 and Soluplus® as carrier materials. The SDs and physical mixtures were characterized by Fourier transform infrared spectroscopy, thermogravimetric analysis, differential scanning calorimetry, X-ray diffractometry, scanning electron microscopy, particle size, specific surface area, pore volume and dissolution profile. The effects of different polymers on the physicochemical properties and dissolution behavior of AG-SDs were studied.

## MATERIAL AND METHODS

### Material

Andrographolide (AG), polyethylene glycol 8000 (PEG8000), poloxamer 188 and polyvinylpyrrolidone K30 (PVPK30) were purchased from Hao-Xuan Biotechnology Co., Ltd (Xi'an, China), MP Biomedical Co., Ltd. (Santa Ana, Cali., USA), Chineway Pharmaceutical Technology Co., Ltd. (Shanghai, China) and Sinopharm Chemical Reagent Co., Ltd. (Shanghai, China), respectively. Soluplus® was kindly gifted from BASF SE (Germany).

### Methods

#### *Preparation of AG-SD by spray drying method*

The spray-drying process was performed using a B-290 mini spray dryer (Büchi, Flawil, Switzerland). All spray-dried powders were obtained from solutions of AG and carrier material in 80% ethanol. The mass ratio of AG and carrier material was 1:3 (Zhao *et al.*, 2019). The spray-dryer inlet temperature was set at 40 °C, the pump rate was 2 mL/min, and the aspirator was set at 100% and the N2 flow at 40 m<sup>3</sup>/h. The powder was collected,

and then stored in a desiccator at room temperature for characterization and dissolution. The prepared SDs were denoted as AG-PEG8000-SD, AG-Poloxamer188-SD, AG-PVPK30-SD and AG-Soluplus®-SD, respectively.

#### *Preparation of physical mixture (PM)*

Appropriate quantities of AG and carrier material with mass ratio of 1:3 were ground together using a pestle and mortar, and then sieved by a standard sieve (60 mesh) to produce a physical mixture. The prepared physical mixtures were denoted as AG-PEG8000-PM, AG-P188-PM, AG-PVPK30-PM, and AG-Soluplus®-PM, respectively.

#### *Fourier transform infrared spectroscopy (FT-IR)*

FT-IR spectra were obtained using a Spectrum Two FT-IR spectrometer (PerkinElmer Corp., USA). About 2–3 mg of the sample was mixed with dry KBr. The powder was compressed in a hydraulic press to form a disc by a powder compressing instrument (FW-4A, Uncommon, Tianjin, China) for FT-IR analysis. The spectra of samples were scanned over a frequency range of 4000–400  $\text{cm}^{-1}$  with a resolution of 4  $\text{cm}^{-1}$ .

#### *Thermogravimetric (TG) analysis*

TG analysis was carried out using a TG/DTA6300 thermal analysis instrument (SII Nano Technology Inc., Tokyo, Japan). Approximately 5 mg sample were placed in aluminum pans and heated from 30 to 500 °C with a heating rate of 10 °C/min.

#### *Differential scanning calorimetry (DSC)*

DSC curves were obtained by a Diamond DSC instrument (PerkinElmer Corp., Waltham, Massachusetts, USA). Calibration of the DSC instrument was carried out using indium as standard. Samples of 5 mg were loaded in aluminum pans and placed into DSC cell. Thermal analysis of samples was carried out at a scanning rate of 10 °C/min in the purge gas of nitrogen, over a temperature range of 20 - 270 °C.

#### *X-ray diffraction (XRD)*

XRD patterns were collected on a D8 ADVANCE-D8X X-ray diffractometer (Bruker AXS GMBH, Karlsruhe, Germany) with a Cu K $\alpha$  line as the source of radiation ( $\lambda = 1.541 \text{ \AA}$ ). Standard runs were carried out using a voltage of 40 kV, a current of 40 mA, and a scanning rate of 8 °/min over a  $2\theta$  range of 5 – 55° with a step size of 0.02°. The same sample of alpha-alumina as an external standard was also scanned in order to correct for the fluctuations in detector responses.

#### *Scanning electron microscope (SEM)*

SEM images were recorded on a Quanta 250 scanning electron microscope (FEI Corp., Hillsboro, Oregon, USA). The samples were mounted on an aluminum stub with double-sided adhesive tape and coated under a vacuum with gold in an argon atmosphere prior to the observation.

#### *Specific surface area and pore volume*

The specific surface area and pore volume were determined by nitrogen gas absorption based on the Brunauer-Emmett-Teller method (Sousa, Sousa, 2002) using TriStar3000 surface area and pore volume analyzer (Micromeritics Instrument Corp., Atlanta, Georgia, USA). The amount of nitrogen adsorbed was measured at partial nitrogen vapor pressure ( $p/p^0$ ), ranging between 0.05 and 0.35. Before measurement, the samples were performed with a continuous nitrogen flow at room temperature overnight to purge out the moisture.

#### *Particle size*

Particle size was measured using a laser diffraction particle size analyser (Mastersizer 2000, Malvern, UK). The intake air pressure and feed rate of the operating parameters of the experiment were 2.5 bars and 55%, respectively. Each sample was tested in triplicates. The particle size quoted in this paper is D[4,3] (the volume weighted mean diameter), D[3,2] (the surface weighted mean diameter), d(0.5) (the diameter corresponding to

50% of the cumulative size distribution) and  $d(0.9)$  (the diameter corresponding to 90% of the cumulative size distribution).

#### *High performance liquid chromatography (HPLC) analysis*

The content of AG was determined using an appropriate HPLC method. The analysis was performed using a 1260 HPLC system (Agilent Corp., Palo Arto, California, USA). The column was Yilite C18 (150 mm  $\times$  4.6 mm, 5  $\mu$ m). The mobile phases were methanol and water (60:40, v:v), the flow rate was 1 mL/min, the column temperature was 30 °C, and the wavelength of the UV detector was 225 nm. This method for determination of AG was validated by the methodological study in the preliminary experiment.

#### *Dissolution testing*

The dissolution testing was tested using Pharmacopoeia of China (Chinese Pharmacopoeia Commission, 2015) type 2 dissolution testing apparatus (paddle method). A ZRS-8G dissolution tester (Tianda-Tianfa Technology Co., Ltd., Tianjin, China) was used in this study. The samples were accurately weighed (0.10 g) and put into the vessels with 900 mL double distilled water ( $n = 6$ ); paddle speed was 100 rpm, and temperature was  $37 \pm 0.5$  °C. The dissolution process was monitored

for 2 h, and the 1.5 mL samples were taken at 5, 10, 15, 30, 45, 60, 90, and 120 min and replaced with an equal volume of the same fresh medium. An aliquot of 1.5 mL was filtered through a 0.22  $\mu$ m filter, and the concentration of AG was determined according to the above-mentioned HPLC condition.

## **RESULTS AND DISCUSSION**

### **FT-IR analysis**

IR is a well-established method for characterizing intermolecular interactions such as hydrogen bonding, and has been extensively applied to probe the drug-carrier material interactions in solid dispersion (Shi *et al.*, 2013). Figure 1 showed the FT-IR spectra of pure AG, carrier material, physical mixture and SD. Table I listed the -OH and -C=O peak position of AG in different circumstances. Compared with the corresponding physical mixture, the -C=O peak position of AG was almost unchanged and the -OH peak position of AG was obviously blue-shifted in the AG-PEG8000-SD and AG-Poloxamer188-SD. It was suggested that the hydrogen bond may be formed between -OH of AG and -OH of PEG8000 or Poloxamer188. The AG-PVPK30-SD and AG-Soluplus<sup>®</sup>-SD showed the significant shift of -C=O and -OH peak position of AG, indicating that both -C=O and -OH of AG may have intermolecular interactions with PVPK30 or Soluplus<sup>®</sup>.

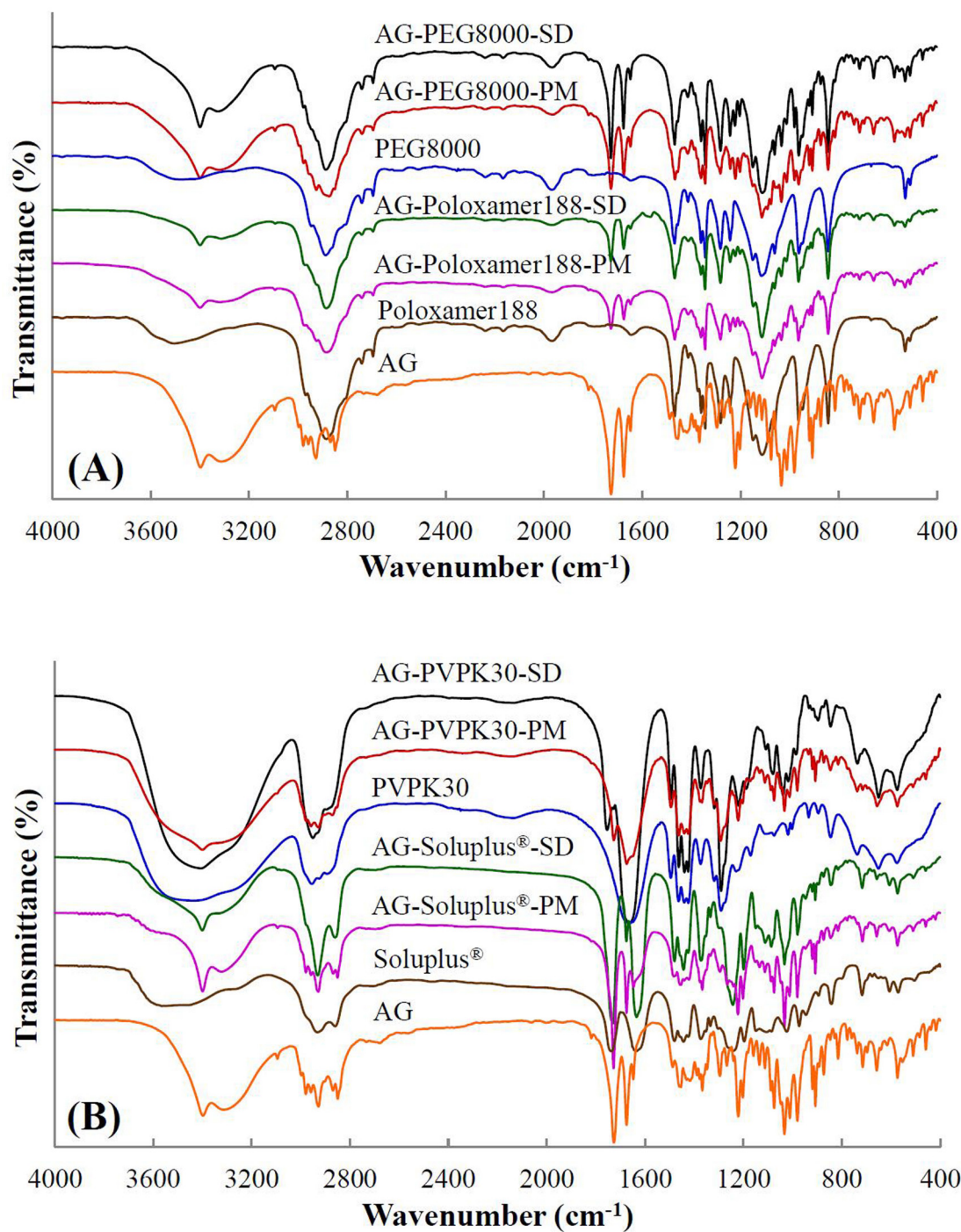


**FIGURE 1** - FT-IR spectra of pure andrographolide (AG), carrier material, physical mixture (PM) and solid dispersion (SD) (A) PEG8000 and Poloxamer188 as carrier materials, (B) PVPK30 and Soluplus<sup>®</sup> as carrier materials.

**TABLE I** - -OH and -C=O peak position of AG in pure AG, PM and SD

Sample	-OH peak position (cm <sup>-1</sup> )	-C=O peak position (cm <sup>-1</sup> )
AG	3397.4, 3313.3	1726.8, 1675.0
AG-PEG8000-PM	3398.3, 3321.5	1727.0, 1674.9
AG-PEG8000-SD	3399.3, 3326.2	1727.1, 1675.8
AG-Poloxamer188-PM	3398.5, 3314.3	1727.2, 1674.5
AG-Poloxamer188-SD	3399.2, 3317.7	1727.2, 1675.0
AG-PVPK30-PM	3399.7, —	1726.9, 1674.6
AG-PVPK30-SD	3405.8, —	1754.4, 1662.8
AG-Soluplus <sup>®</sup> -PM	3399.1, 3325.4	1728.2, 1675.0
AG-Soluplus <sup>®</sup> -SD	3405.5, —	1737.3, 1675.0

AG is andrographolide, PM is physical mixture, SD is solid dispersion.

### TG analysis

TG analysis can be used to compare the thermal stability of SD and physical mixture (Albadarin *et al.*, 2017; Veronez *et al.*, 2015; Lim *et al.*, 2013). The TG curves and 5% weight-loss temperature ( $T_i$ ) of samples were shown in Figure 2 and Table II, respectively. As shown in Table II, the  $T_i$  of AG-PEG8000/Poloxamer188-PM and AG-PEG8000/Poloxamer188-SD was higher than that of pure AG, in contrast to the  $T_i$  of AG-PVPK30/Soluplus<sup>®</sup>-PM and AG-PVPK30/

Soluplus<sup>®</sup>-SD was lower than that of pure AG. This is due to the fact that PEG8000 and Poloxamer188 are semicrystalline polymers with higher  $T_i$ , and PVPK30 and Soluplus<sup>®</sup> are amorphous polymers, and their  $T_i$  are lower than that of pure AG. Therefore, the thermal stability of AG-PEG8000-SD and AG-Poloxamer188-SD was better than that of AG-PVPK30-SD and AG-Soluplus<sup>®</sup>-SD. Moreover, the  $T_i$  of all AG-SDs was obviously smaller than that of their respective AG-physical mixture, which indicated that the crystallinity of AG in AG-SDs decreased.

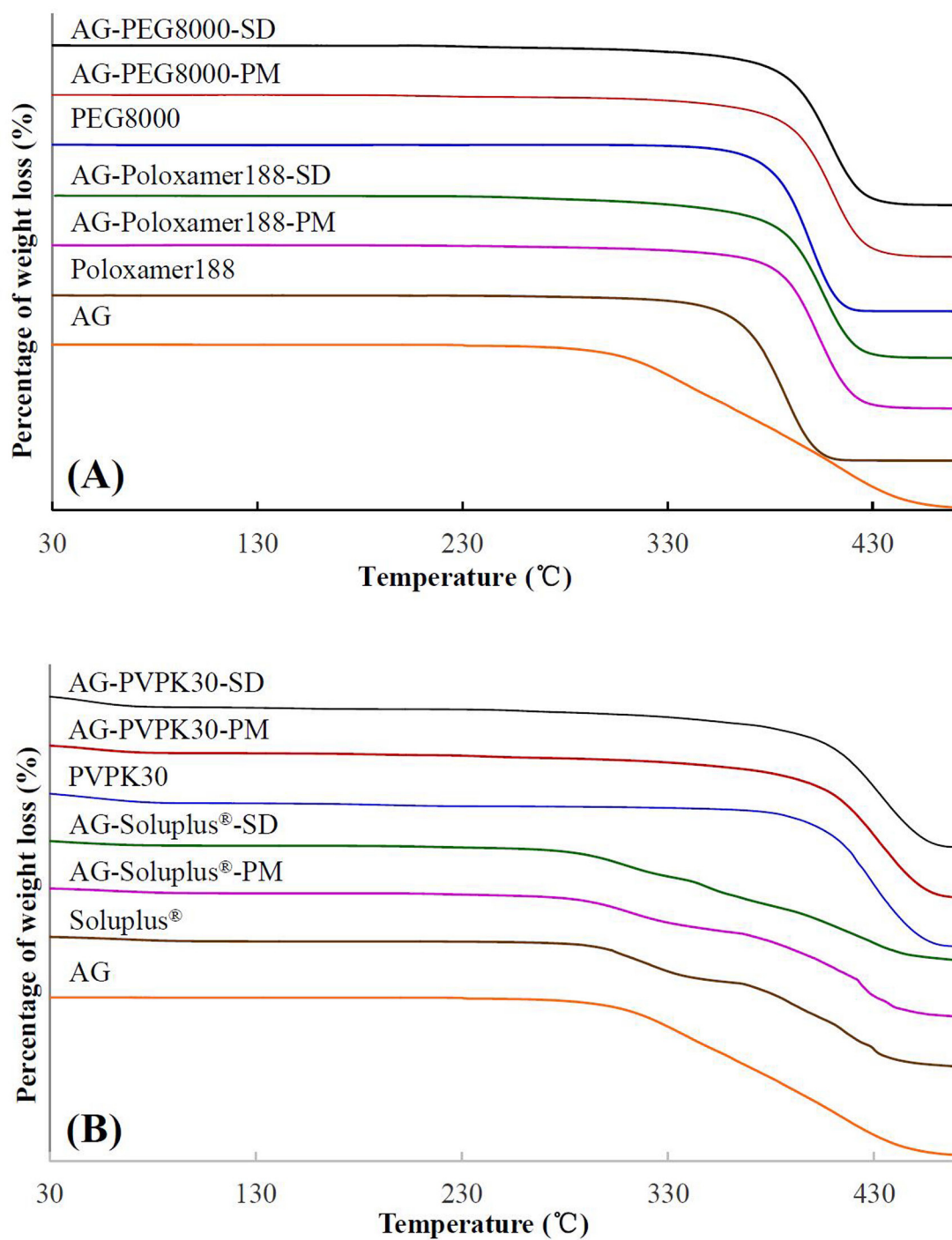


**FIGURE 2** - TG curves of pure andrographolide (AG), carrier material, physical mixture (PM) and solid dispersion (SD) (A) PEG8000 and Poloxamer188 as carrier materials, (B) PVPK30 and Soluplus® as carrier materials.

**TABLE II** -  $T_i$  and  $T_m$  of pure AG, carrier material, PM and SD

Sample	$T_i$ (°C)	$T_m$ (°C)	Sample	$T_i$ (°C)	$T_m$ (°C)
AG	299.6	243.7			
PEG8000	363.0		Poloxamer188	340.2	
PVPK30	64.5		Soluplus <sup>®</sup>	287.1	
AG-PEG8000-PM	352.0	217.7	AG-Poloxamer188-PM	345.4	224.4
AG-PEG8000-SD	341.8	209.0	AG-Poloxamer188-SD	326.8	222.4
AG-PVPK30-PM	74.2	238.4	AG-Soluplus <sup>®</sup> -PM	267.5	232.0
AG-PVPK30-SD	54.0	—	AG-Soluplus <sup>®</sup> -SD	255.5	—

AG is andrographolide, PM is physical mixture, SD is solid dispersion.

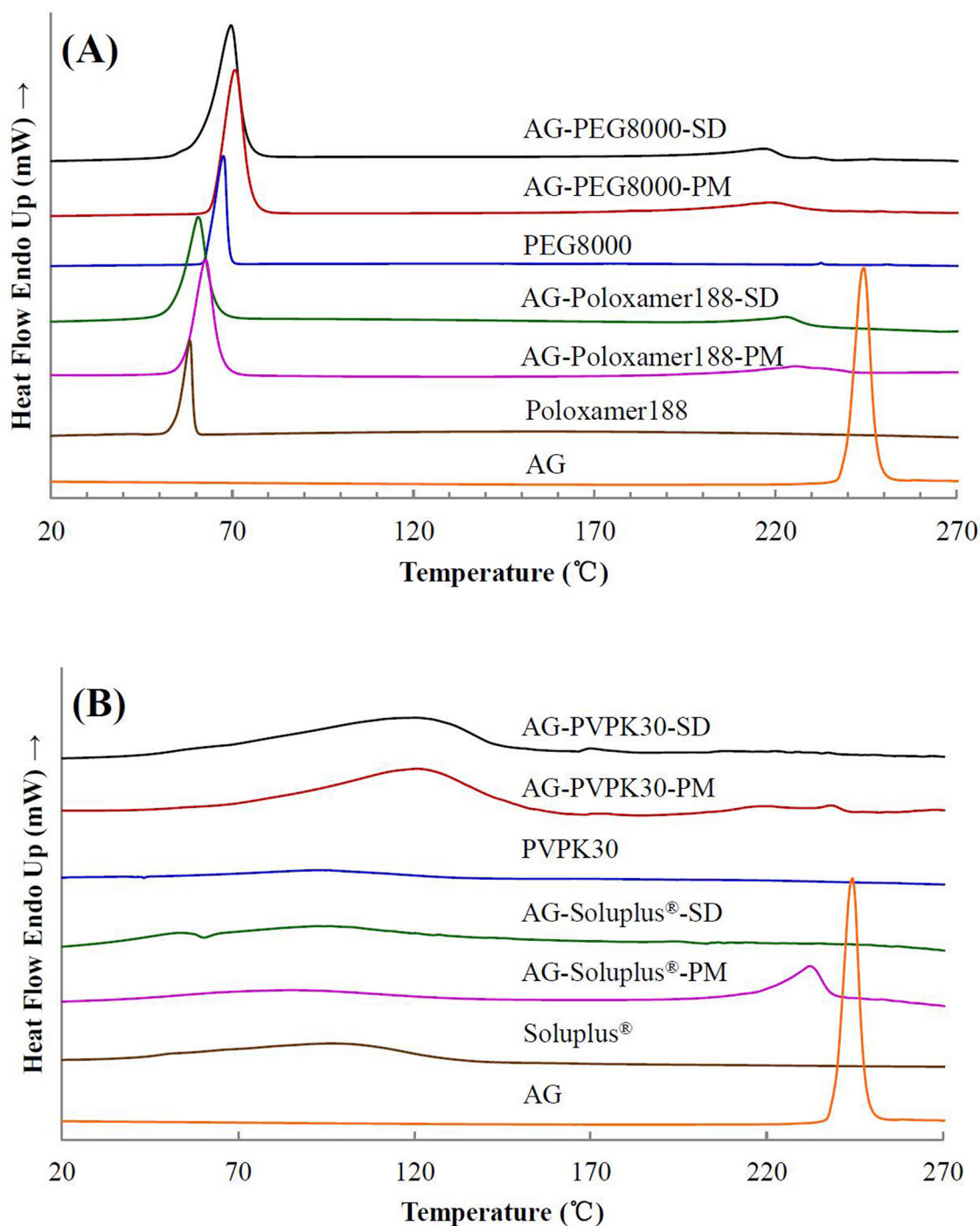
### DSC analysis

Figure 3 showed the DSC thermograms of pure AG, carrier materials, physical mixture and SD. Table II listed the melting temperature ( $T_m$ ) of all the samples near 200 - 250 °C. As shown in Figure 3, the DSC thermogram of pure AG exhibited a sharp endothermic peak at 243 °C, indicating AG is typical crystalline substance.

There was no sharp endothermic peak of crystal AG in AG-PEG8000-PM and AG-Poloxamer188-PM, but a weakened endothermic peak at 218 °C and 224 °C, respectively, which was close to the endothermic peak of the corresponding SD. This was because, during the heating of measuring DSC curve the carrier material firstly melted, and then the crystal AG was partially dissolved in melted carrier material and formed SD.

Therefore, the  $T_m$  of the physical mixture was similar to that of the corresponding SD. In AG-PEG8000-SD and AG-Poloxamer188-SD, a small endothermic peak was observed at 209 °C and 222 °C, respectively (Figure 3 and Table II). This result indicated that the completely amorphous AG-PEG8000-SD and AG-Poloxamer188-SD had not been obtained. The AG was in a partial-amorphous and partial-crystal state in the AG-PEG8000-SD and AG-Poloxamer188-SD.

The melting peak of typical crystal AG was observed at 232 °C for AG-Soluplus<sup>®</sup>-PM, and a small endothermic peak for AG-PVPK30-PM at 238 °C. Compared with the corresponding physical mixture, all the AG-PVPK30-SD and AG-Soluplus<sup>®</sup>-SD did not appear the melting peaks of AG.



**FIGURE 3** - DSC thermograms of pure andrographolide (AG), carrier material, physical mixture (PM) and solid dispersion (SD) (A) PEG8000 and Poloxamer188 as carrier materials, (B) PVPK30 and Soluplus<sup>®</sup> as carrier materials.

### XRD analysis

The crystallinity of pure AG, carrier materials, physical mixture and SD were examined using XRD

and their diffraction patterns were displayed in Figure 4. The AG diffraction pattern demonstrated that it has a very crystalline nature with sharp intensive peaks throughout its pattern. The crystalline AG characteristic

diffraction peaks have been observed in all the physical mixtures.

Comparing the SD and corresponding physical mixture XRD patterns, demonstrated that the AG-PEG8000-SD and AG-Poloxamer188-SD have sharp diffraction peaks associated with AG, suggesting that the AG had retained some of its crystalline nature. However, the intensity of AG diffraction peaks in the AG-PEG8000-SD and AG-Poloxamer188-SD reduced significantly more than that in

the corresponding physical mixture. This indicated that the AG was in a partial-amorphous and partial-crystalline state in the AG-PEG8000-SD and AG-Poloxamer188-SD. AG-PVPK30-SD had the AG very weak diffraction peaks at  $2\theta$  12.09° and 15.75°, which imply that a small amount of crystalline AG still existed in this SD. AG-Soluplus®-SD had no diffraction peaks associated with AG and thus would suggest that the AG in this SD was completely in its amorphous state.

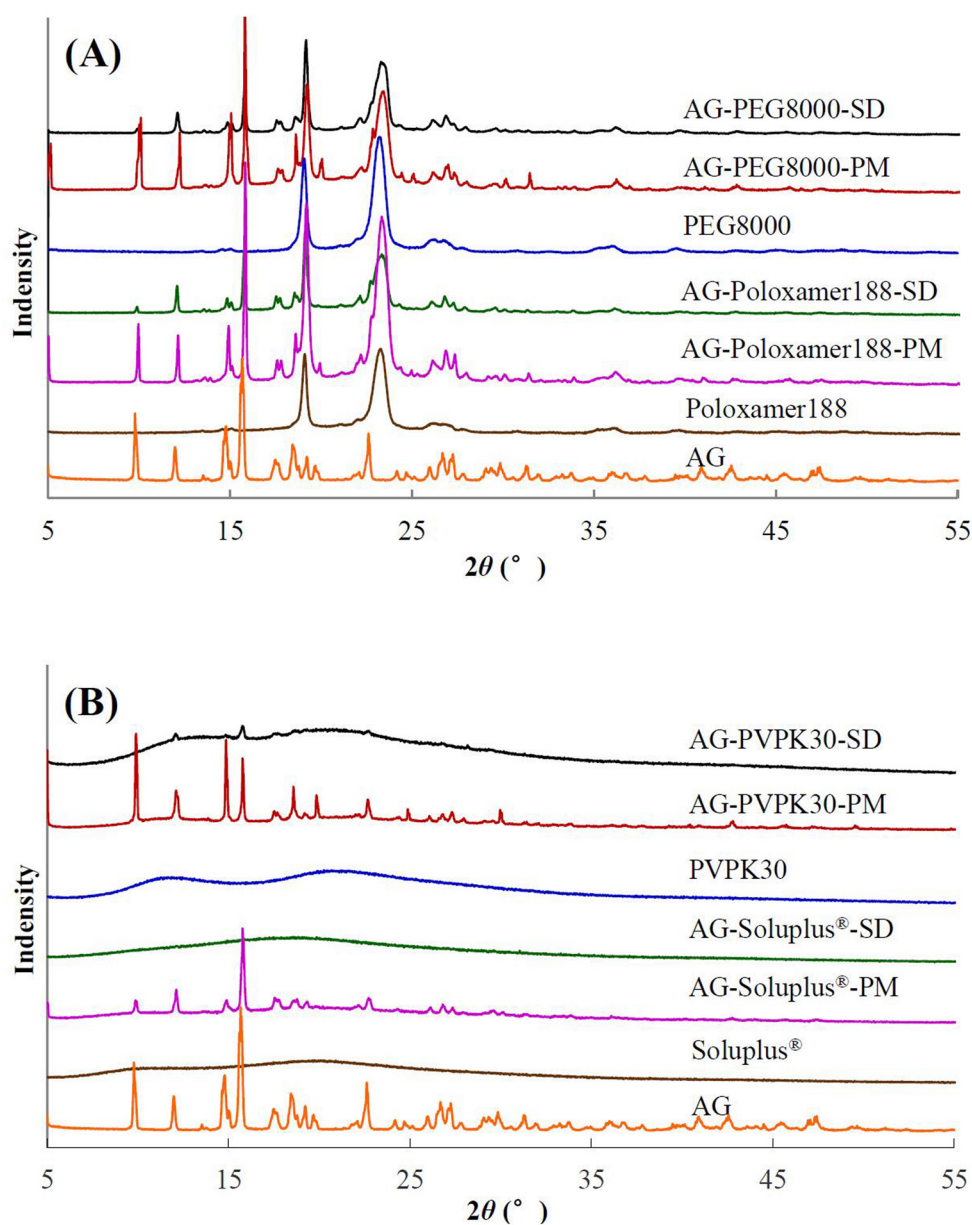


**FIGURE 4** - XRD patterns of pure andrographolide (AG), carrier material, physical mixture (PM) and solid dispersion (SD) (A) PEG8000 and Poloxamer188 as carrier materials, (B) PVPK30 and Soluplus® as carrier materials.

XRD pattern demonstrated a small amount of crystalline AG still existed in the AG-PVPK30-SD. However, the AG melting peak in AG-PVPK30-SD was not found by DSC analysis. This may be due to PVPK30 firstly melted during the heating of measuring DSC curve, and then a small amount of crystal AG was dissolved in melted carrier material. Therefore, no AG melting peak in AG-PVPK30-SD was detected in DSC analysis. The results of DSC and XRD analysis showed that the AG crystallinity in AG-PVPK30-SD and AG-Soluplus<sup>®</sup>-SD was significantly lower than that in AG-PEG8000-SD and AG-Poloxamer188-SD.

### **SEM analysis**

In order to determine the morphology of SDs, SEM analysis of the samples was performed. As illustrated in Figure 5a, pure AG showed block crystalline structure with a smooth surface. In physical mixtures the AG and carrier material displayed their original surface morphology. The surface morphology of AG-SDs prepared with different polymers as carrier material had obvious differences: the powders of AG-PEG8000-SD and AG-Poloxamer188-SD were rod particles with irregular protuberances, and the particle size was large; the powders of AG-PVPK30-SD and AG-Soluplus<sup>®</sup>-SD were spherical particles with small particle size. AG-PVPK30-SD was a spherical particle with a smooth surface (Figure 5M), and AG-Soluplus<sup>®</sup>-SD was a flat spherical particle with middle depression (Figure 5Q).

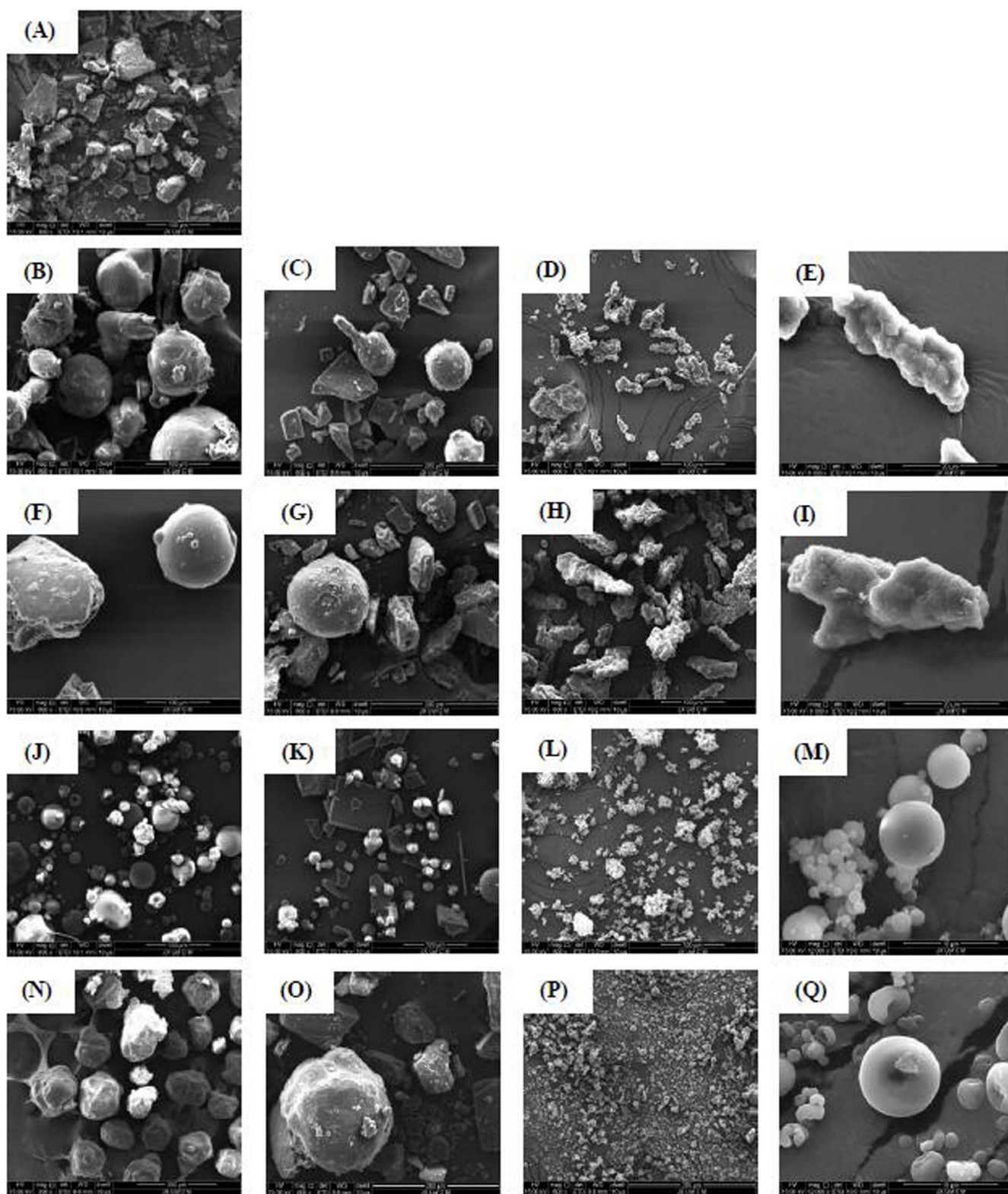


**FIGURE 5**- SEM photographs of samples: (A) AG, (B) PEG8000, (C) AG-PEG8000-PM, (D) AG-PEG8000-SD, (E) AG-PEG8000-SD, (F) Poloxamer188, (G) AG-Poloxamer188-PM, (H) AG-Poloxamer188-SD, (I) AG-Poloxamer188-SD, (J) PVPK30, (K) AG-PVPK30-PM, (L) AG-PVPK30-SD, (M) AG-PVPK30-SD, (N) Soluplus®, (O) AG-Soluplus®-PM, (P) AG-Soluplus®-SD, (Q) AG-Soluplus®-SD.

### Particle size, specific surface area and pore volume

Table III listed the particle size, specific surface area and pore volume of all the SDs and physical mixtures. Compared with the corresponding physical mixture, the particle size of AG-SD decreased, the specific surface area and the pore volume increased. These changes in the powder properties can significantly increase the effective contact area between the SD powder and the dissolution medium, which was beneficial to the AG dissolution in AG-SD.

In order to further study the effect of different polymers on the powder properties of AG-SDs, cluster analysis was carried out on all SDs. Based on the variable of surface weighted mean diameter ( $D[3,2]$ ), volume weighted meandiameter ( $D[4,3]$ ),  $d_{0.5}$ ,  $d_{0.9}$ , surface

area, pore volume and pore size, the samples were cluster analyzed by intergroup connection clustering method and squared Euclidean distance measured data. The cluster analysis Figure 6 was calculated by SPSS19.0 software. As can be seen from Figure 6, when the distance was less than 25, the samples can be divided into two groups: the AG-Poloxamer188-SD was the first group; the other SDs were the second group. When the distance was reduced to less than 4, AG-PEG8000-SD was isolated from the second group in a single group. Considering the results of this cluster analysis and above SEM photographs, it was shown that there were significant differences in the surface morphology, surface area and particle size between AG-PEG8000/ Poloxamer188-SDs and AG-PVPK30/Soluplus<sup>®</sup>-SD.

**TABLE III** - Particle size, specific surface area and pore volume of SD and PM

Sample	D[3,2] ( $\mu\text{m}$ )	D[4,3] ( $\mu\text{m}$ )	$d_{0.5}$ ( $\mu\text{m}$ )	$d_{0.9}$ ( $\mu\text{m}$ )	Specific surface area ( $\text{m}^2/\text{g}$ )	Pore volume ( $\times 10^{-3}$ , $\text{m}^3/\text{g}$ )	Pore size ( $\text{\AA}$ )
AG-PEG8000-SD	25.9 $\pm$ 1.8	168.1 $\pm$ 11.2	42.8 $\pm$ 2.9	557.4 $\pm$ 35.6	0.4370 $\pm$ 0.0331	1.241 $\pm$ 0.0933	113.6 $\pm$ 8.3
AG-PEG8000-PM	52.5 $\pm$ 4.3	161.8 $\pm$ 15.4	145.5 $\pm$ 15.1	322.9 $\pm$ 28.3	0.0109 $\pm$ 0.0987	1.034 $\pm$ 0.0987	3783.1 $\pm$ 305.9
AG-Poloxamer188-SD	51.8 $\pm$ 3.7	154.1 $\pm$ 10.9	79.6 $\pm$ 6.6	337.3 $\pm$ 26.0	0.1984 $\pm$ 0.0009	0.634 $\pm$ 0.0454	127.7 $\pm$ 9.5
AG-Poloxamer188-PM	59.1 $\pm$ 6.0	198.0 $\pm$ 18.6	181.8 $\pm$ 20.1	389.7 $\pm$ 39.1	0.0061 $\pm$ 0.0136	0.627 $\pm$ 0.0622	4100.7 $\pm$ 397.7
AG-PVPK30-SD	3.9 $\pm$ 0.2	21.6 $\pm$ 1.9	4.9 $\pm$ 0.4	59.8 $\pm$ 5.1	1.9101 $\pm$ 0.1341	4.862 $\pm$ 0.3265	101.8 $\pm$ 8.4
AG-PVPK30-PM	29.0 $\pm$ 2.2	103.1 $\pm$ 9.5	52.7 $\pm$ 5.1	148.0 $\pm$ 12.3	0.0360 $\pm$ 0.0040	0.185 $\pm$ 0.0138	172.4 $\pm$ 15.6
AG-Soluplus <sup>®</sup> -SD	3.2 $\pm$ 0.2	4.6 $\pm$ 0.3	3.9 $\pm$ 0.2	8.4 $\pm$ 0.4	0.7292 $\pm$ 0.0659	2.673 $\pm$ 0.1711	146.6 $\pm$ 8.2
AG-Soluplus <sup>®</sup> -PM	62.3 $\pm$ 4.1	287.3 $\pm$ 20.1	283.2 $\pm$ 18.9	510.3 $\pm$ 41.5	0.0294 $\pm$ 0.0027	0.132 $\pm$ 0.0092	180.2 $\pm$ 15.0

$D[3,2]$  is surface weighted mean diameter,  $D[4,3]$  is volume weighted meandiameter,  $d(0.5)$  is the diameter corresponding to 50% of the cumulative size distribution,  $d(0.9)$  is the diameter corresponding to 90% of the cumulative size distribution. PM is physical mixture, SD is solid dispersion.

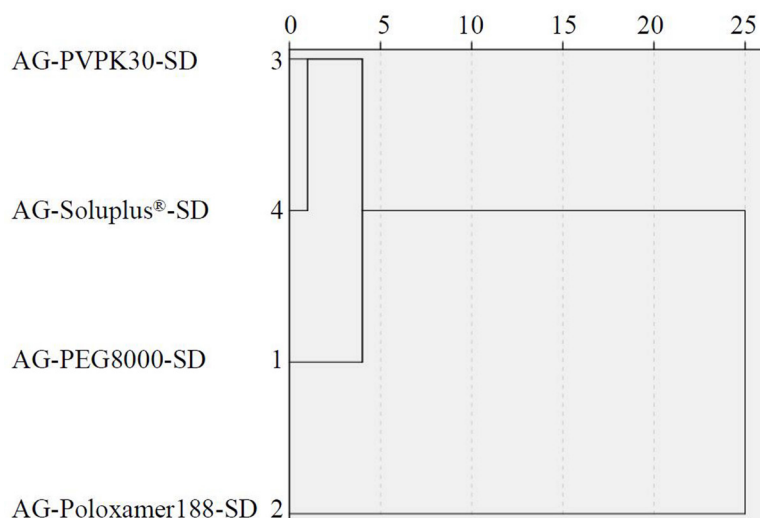


**FIGURE 6** - Cluster analysis tree diagram by intergroup connection on the variable of particle size, specific surface area and pore volume.

### Dissolution testing

The dissolution of a poorly water-soluble drug is crucial where it is the rate-limiting step in the oral absorption process from a solid dosage form and is an important parameter related to bioavailability (Mohammadi *et al.*, 2010; Bothiraja *et al.*, 2009). The dissolution profiles of pure AG, physical mixture and SD were illustrated in Figure 7. It can be seen that the

maximum dissolution percentage of pure AG in 120 min was only 22% when using water as the medium.  $Q_5$ min (the dissolution percentage in 5 min) and  $t_{75\%}$  (time required for 75% dissolution) were calculated and listed in Table IV. As shown in Table IV, all the SDs exhibited higher values of  $Q_5$ min and lower values of  $t_{75\%}$  when compared with the physical mixture and pure AG. The results indicated that the dissolution rate of AG in all the SDs was increased obviously.

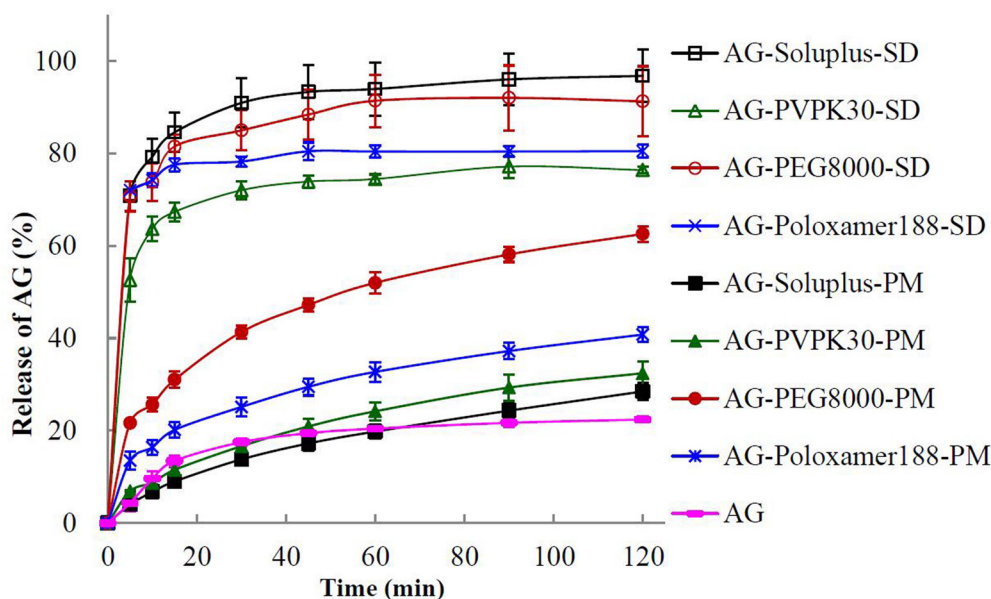


**FIGURE 7** - Dissolution profiles of pure andrographolide (AG), physical mixture (PM) and solid dispersion (SD) ( $n = 6$ ).

**TABLE IV** -  $Q_{5\min}$  and  $t_{75\%}$  of pure AG, PM and SD

Sample	$Q_{5\min}$ (%)	$t_{75\%}$ (min)
AG	4.32±1.84	>120
AG-PEG8000-PM	21.65±0.40	>120
AG-PEG8000-SD	70.73±3.23	11
AG-Poloxamer188-PM	13.47±1.99	>120
AG-Poloxamer188-SD	72.07±1.45	11
AG-PVPK30-PM	6.88±0.19	>120
AG-PVPK30-SD	52.61±4.71	66
AG-Soluplus <sup>®</sup> -PM	3.99±0.47	>120
AG-Soluplus <sup>®</sup> -SD	82.56±0.86	4

AG is andrographolide, PM is physical mixture, SD is solid dispersion.

In order to further study the effect of different polymers on the dissolution behavior of AG in the SD, all the samples were investigated by cluster analysis. Based on the variable of the dissolution percentage of AG at different time, the samples were cluster analyzed by intergroup connection clustering method and squared Euclidean distance measured data. The cluster analysis Figure 8 was calculated by SPSS19.0 software. As can be seen from Figure 8 when the distance was less than 25, the samples can be divided into two groups: the physical mixtures and pure AG were the first group; the SDs were the second group. The results suggested that SD prepared

with different polymers can significantly improve the dissolution of AG.

When the distance was less than 2, the SDs were further divided into two groups: AG-Poloxamer188-SD and AG-PVPK30-SD were the first group, AG-PEG8000-SD and AG-Soluplus<sup>®</sup>-SD were the second group. The dissolution percentage of AG in AG-Poloxamer188-SD and AG-PVPK30-SD at 120 min was only 80.51% and 76.41%, respectively, which was due to the presence of partial-crystalline AG in both SDs. Moreover, in the process of dissolution the powder of AG-PVPK30-SD was swelled and water film was formed on its surface, which prevented the diffusion of AG from SD powder to the dissolution medium. The surface area and pore volume of AG-Poloxamer188-SD were the smallest among the SDs, which reduced its effective contact area with the dissolution medium. The above factors reduced the dissolution rate of AG in AG-Poloxamer188-SD and AG-PVPK30-SD.

The AG in AG-Soluplus<sup>®</sup>-SD was completely amorphous. The powder of AG-Soluplus<sup>®</sup>-SD had a larger specific surface area and pore volume, and water can easily enter into the SD. These were beneficial to the dissolution of AG. It was worth noting that the AG was in a partial-amorphous and partial-crystalline state in AG-PEG8000-SD, and the specific surface area and pore volume of AG-PEG8000-SD were much smaller than those of AG-Soluplus<sup>®</sup>-SD. However, because of the good hydrophilicity and wetting of PEG8000, the cumulative dissolution percentage of AG in AG-PEG8000-SD at 120 min was up to 91.30%.

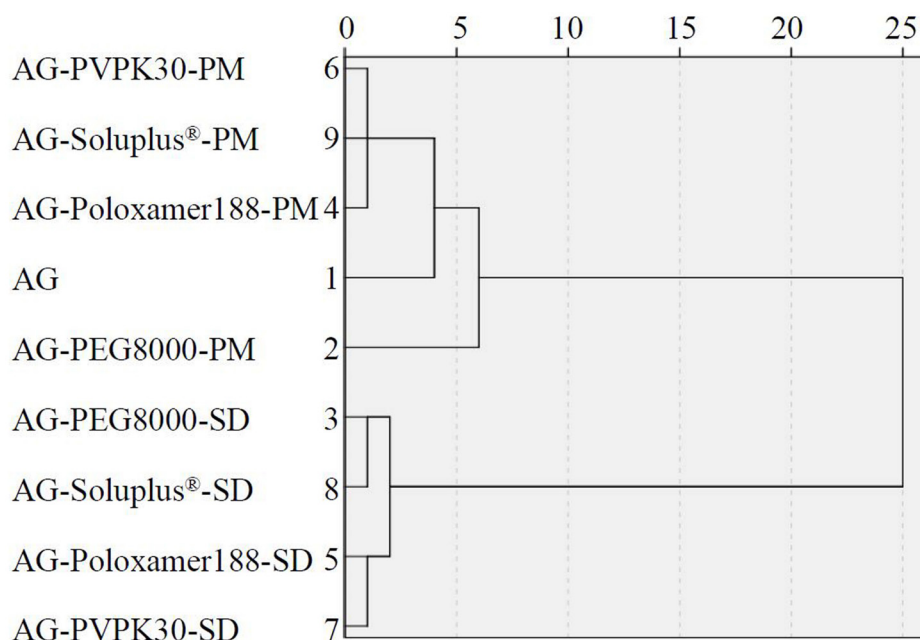


**FIGURE 8** - Cluster analysis tree diagram by intergroup connection on the variable of the dissolution percentage at different time.

In this paper, the AG-SDs were prepared by the spray-drying method, using PEG8000, Poloxamer188, PVPK30 and Soluplus® as carrier materials. The results showed that there were obvious differences in intermolecular interaction, thermal stability, drug crystallinity, surface morphology, specific surface area, pore volume and particle size and dissolution behavior of the AG-SDs prepared using different polymer as carrier material. Compared with AG-Soluplus®-SD, AG in AG-PEG8000-SD was a partial-crystalline and partial-amorphous state, and its specific surface area and pore volume were smaller, but AG-PEG8000-SD powder was easy to wetting and did not swell when it was in contact with dissolved medium. Therefore, the dissolution profile of AG in AG-PEG8000-SD was similar to that in AG-Soluplus®-SD. Soluplus® and PEG8000 were suitable polymers to design AG-SDs in this research considering both physicochemical properties and dissolution behaviors. The results of this work suggested that when selecting carrier materials for SD, we should not only consider the state of drugs in SD and the powder properties of SD, but also consider whether there is swelling when the carrier materials are in contact with the dissolution medium.

## ACKNOWLEDGEMENTS:

This research was supported by the Science and Technology Research Project of Education Department of Jiangxi Provincial of China (No GJJ201233); the National Natural Science Foundation of China (No 81560654); the Health and Family Planning Commission of Jiangxi Provincial of China (No 2015A055); Jiangxi University of Chinese Medicine Science and Technology Innovation Team Development Program.

## REFERENCES

- Albadarin AB, Potter CB, Davis MT, Iqbal J, Korde S, Pagire S, et al. Development of stability-enhanced ternary solid dispersions via combinations of HPMCP and Soluplus® processed by hot melt extrusion. *Int J Pharm.* 2017;532(1):603-11.
- Barmpalexis P, Koutsidis I, Karavas E, Louka D, Papadimitriou SA, Bikiaris DN. Development of PVP/PEG mixtures as appropriate carriers for the preparation of drug solid dispersions by melt mixing technique and optimization of dissolution using artificial neural networks. *Eur J Pharm Biopharm.* 2013;85(3):1219-31.
- Bhardwaj V, Trasi NS, Zemlyanov DY, Taylor LS. Surface area normalized dissolution to study differences in itraconazole-

- copovidone solid dispersions prepared by spray-drying and hot melt extrusion. *Int J Pharm.* 2018;540(1-2):106-19.
- Bikiaris D, Papageorgiou GZ, Stergiou A, Pavlidou E, Karavas E, Kanaze F, et al. Physicochemical studies on solid dispersions of poorly water-soluble drugs - Evaluation of capabilities and limitations of thermal analysis techniques. *Thermochim Acta.* 2005;439(1-2):58-67.
- Bothiraja C, Shinde MB, Rajalakshmi S, Pawar AP. Evaluation of molecular pharmaceutical and in-vivo properties of spray-dried isolated andrographolide-PVP. *J Pharm Pharmacol.* 2009;61(11):1465-72.
- Calabrese C, Berman SH, Babish JG, Ma X, Shinto L, Dorr M, et al. A phase I trial of andrographolide in HIV positive patients and normal volunteers. *Phytother Res.* 2000;14(5):333-8.
- Chiou WL, Riegelman S. Pharmaceutical applications of solid dispersion systems. *J Pharm Sci.* 1971;60(9):1281-302.
- Chokshi RJ, Zia H, Sandhu HK, Shah NH, Malick WA. Improving the dissolution rate of poorly water soluble drug by solid dispersion and solid solution: pros and cons. *Drug Deliv.* 2007;14(1): 33-45.
- Chutimaworapan S, Ritthidej GC, Yonemochi E, Oguchi T, Yamamoto K. Effect of water-soluble carriers on dissolution characteristics of nifedipine solid dispersions. *Drug Dev Ind Pharm.* 2000;26(11):1141-50.
- Eloy JO, Marchetti JM. Solid dispersions containing ursolic acid in Poloxamer 407 and PEG 6000: A comparative study of fusion and solvent methods. *Powder Technol.* 2014;253:98-106.
- FDA. Waiver of in vivo bioavailability and bioequivalence studies for immediate-release solid oral dosage forms based on a biopharmaceutics classification system. Guidance for Industry. 2000.
- Hu XY, Lou H, Hageman MJ. Preparation of lapatinib ditosylate solid dispersions using solvent rotary evaporation and hot melt extrusion for solubility and dissolution enhancement. *Int J Pharm.* 2018;552(1-2):154-63.
- Jiang Y, Wang F, Xu H, Liu H, Meng Q, Liu W. Development of andrographolide loaded PLGA microspheres: optimization, characterization and in vitro-in vivo correlation. *Int J Pharm.* 2014;475(1-2):475-84.
- Kawabata Y, Wada K, Nakatani M, Yamada S, Onoue S. Formulation design for poorly water-soluble drugs based on biopharmaceutics classification system: basic approaches and practical applications. *Int J Pharm.* 2011;420(1):1-10.
- Lim RTY, Ng WK, Tan RBH. Dissolution enhancement of indomethacin via amorphization using co-milling and supercritical co-precipitation processing. *Powder Technol.* 2013;240:79-87.
- Mahmah O, Tabbakh R, Kelly A, Paradkar A. A comparative study of the effect of spray drying and hot-melt extrusion on the properties of amorphous solid dispersions containing felodipine. *J Pharm Pharmacol.* 2014;66(2):275-84.
- Marasini N, Tran TH, Poudel BK, Cho HJ, Choi YK, Chi SC, et al. Fabrication and evaluation of pH-modulated solid dispersion for telmisartan by spray-drying technique. *Int J Pharm.* 2013;441(1-2):424-32.
- Matsuda T, Kuroyanagi M, Sugiyama S, Umehara K, Ueno A, Nishi K. Cell differentiation-inducing diterpenes from *Andrographis paniculata* Nees. *Chem Pharm Bull (Tokyo).* 1994;42(6):1216-25.
- Mohammadi G, Barzegar-Jalali M, Valizadeh H, Nazemiyeh H, Barzegar-Jalali A, Siahi Shadbad MR, et al. Reciprocal powered time model for release kinetic analysis of ibuprofen solid dispersions in oleaster powder, microcrystalline cellulose and crospovidone. *J Pharm Pharm Sci.* 2010;13(2):152-61.
- Ramadhani N, Shabir M, McConville C. Preparation and characterisation of Kolliphor® P 188 and P 237 solid dispersion oral tablets containing the poorly water soluble drug disulfiram. *Int J Pharm.* 2014;475(1-2):514-22.
- Reginald-Opara JN, Attama A, Ofokansi K, Umeyor C, Kenechukwu. Molecular interaction between glimepiride and Soluplus(R)-PEG 4000 hybrid based solid dispersions: characterisation and anti-diabetic studies. *Int J Pharm.* 2015;496(2):741-750.
- Sermkaew N, Ketjinda W, Boonme P, Phadoongsombut N, Wiwattanapatapee R. Liquid and solid self-microemulsifying drug delivery systems for improving the oral bioavailability of andrographolide from a crude extract of *Andrographis paniculata*. *Eur J Pharm Sci.* 2013;50(3-4):459-66.
- Shen YC, Chen CF, Chiou WF. Andrographolide prevents oxygen radical production by human neutrophils: possible mechanism(s) involved in its anti-inflammatory effect. *Br J Pharmacol.* 2002;135(2):399-406.
- Shi NQ, Lei YS, Song LM, Yao J, Zhang XB, Wang XL. Impact of amorphous and semicrystalline polymers on the dissolution and crystallization inhibition of pioglitazone solid dispersions. *Powder Technol.* 2013;247:211-21.
- Singha PK, Roy S, Dey S. Protective activity of andrographolide and arabinogalactan proteins from *Andrographis paniculata* Nees. against ethanol-induced toxicity in mice. *J Ethnopharmacol.* 2007;111(1):13-21.
- Singh G, Kaur L, Gupta GD, Sharma S. Enhancement of the solubility of poorly water soluble drugs through solid

dispersion: a comprehensive review. *Indian J Pharm Sci.* 2017;79(5):674-87.

Sousa JJ, Sousa A, Podczeczek F, Newton JM. Factors influencing the physical characteristics of pellets obtained by extrusion-spheronization. *Int J Pharm.* 2002;232(1-2):91-106.

Thenmozhi K, Yoo YJ. Enhanced solubility of piperine using hydrophilic carrier-based potent solid dispersion systems. *Drug Dev Ind Pharm.* 2017;43(9):1501-9.

Thybo P, Pedersen BL, Hovgaard L, Holm R, Mullertz A. Characterization and physical stability of spray dried solid dispersions of probucol and PVP-K30. *Pharm Dev Technol.* 2008;13(5):375-86.

Thiry J, Lebrun P, Vinassa C, Adam M, Netchacovitch L, Ziemons E, et al. Continuous production of itraconazole-based solid dispersions by hot melt extrusion: Preformulation, optimization and design space determination. *Int J Pharm.* 2016;515(1-2):114-24.

Veronez IP, Daniel JSP, Júnior CEC, Garcia JS, Trevisan MG. Development, characterization, and stability studies of ethinyl estradiol solid dispersion. *J Therm Anal Calorim.* 2015;120(1):573-81.

Vo CL, Park C, Lee BJ. Current trends and future perspectives of solid dispersions containing poorly water-soluble drugs. *Eur J Pharm Biopharm.* 2013;85(3 Pt B):799-813.

Wen L, Xia N, Chen X, Li Y, Hong Y, Liu Y, et al. Activity of antibacterial, antiviral, anti-inflammatory in compounds andrographolide salt. *Eur J Pharmacol.* 2014;740:421-7.

Zhang XF, Tan BK. Antihyperglycaemic and anti-oxidant properties of *Andrographis paniculata* in normal and diabetic rats. *Clin Exp Pharmacol Physiol.* 2000;27(5-6):358-63.

Zhang Y, Hu X, Liu X, Dandan Y, Di D, Yin T, et al. Dry state microcrystals stabilized by an HPMC film to improve the bioavailability of andrographolide. *Int J Pharm.* 2015;493(1-2):214-23.

Zhao GW, Zeng QY, Zhang SD, Zhong YQ, Wang CH, Chen YS, et al. Effect of carrier lipophilicity and preparation method on the properties of andrographolide–solid dispersion. *Pharmaceutics.* 2019;11(2):74-91.

Received for publication on 18<sup>th</sup> December 2019

Accepted for publication on 11<sup>th</sup> August 2020